Simple online algorithm for detecting cow's ECG beat-to-beat interval using a microcontroller

Tiusanen, M. Johannes[1*], Pastell, Matti[2]

(1 Department of Agricultural Sciences, University of Helsinki, P.O Box 28, FI-00014 University of Helsinki, Finland

2 Natural Resources Institute Finland (Luke), Green Technology, Viikinkaari 4, FI-00790, Helsinki, Finland)

Abstract: This paper describes an online algorithm for detecting cow's beat-to-beat interval on a small embedded microcontroller. The target device is an ECG implant which only provides limited calculation power and insufficient storage memory for long term complete ECG data logging. No common computationally efficient method for detecting the human R-wave was found successful for cattle ECG data with the used measurement configuration. Our algorithm detects a cow's S-wave, which is the most distinguishable part of the QRS-complex. The offset and amplitude adaptive algorithm utilizes only arithmetic operations and logic conditions.

1 Introduction

Heart rate variability is recognized as an interesting parameter for studying welfare of cattle (von Borell et al., 2008). It has been used to study for instance the stress level of cows in different milking systems (Gygax et al., 2008; Hagen at al. 2005), temperament of cow (Frondelius et al. 2015), and dehorning pain in calves (Stewart et al., 2009).

However, measuring electrocardiogram (ECG) with surface electrodes in normal production environments is very impractical and the measurements are generally noisy (Chen et al. 2000). Our research group has been working on an implantable ECG device for measuring heart rate variability in dairy cows (Riistama and Vuorela, 2011). The aim of this study was to develop a simple and fast real-time algorithm for detecting beat-to-beat intervals from bovine ECG measured with an implantable device. This would enable the device to only store the interval

times instead of raw ECG reducing the storage space considerably. The implantable measurement device, on which the algorithm will be embedded on, has a 16-bit ultralow power RISC microcontroller running at 8 MHz clock speed (Riistama and Vuorela, 2011).

As the highest possible ADC speed will be 340 Hz, the detector algorithm must execute in much less than 3 ms. This leads to a high demand of simplicity in the algorithm computation. After testing several simple derivative based methods developed for human ECG (Friesen et al. 1990) with poor performance we developed our own method. In more complex existing algorithms the baseline wander is often removed by higher arithmetic methods, such as ensemble averaging, finite impulse response filters or cubic splines (Jane et al., 1992). A derivative high-pass filter is more suitable considering our target application, where peak timing is essential but true voltage values insignificant.

This paper demonstrates the development and operation of the developed algorithm using ECG measured with surface electrodes.

2 Materials and methods

2.1 Data collection

Surface ECG was recorded from 11 cows using portable Embla titanium recorder device that weighed 0.3 kg and measured 12 cm × 8 cm × 3 cm (Embla Titanium, Embla Systems Inc., Broomfield, USA).   The cables, mobile recording device and a counter-weight were fixed to the udder holder on the back of the cow.   Ten curves were recorded at 256 Hz and 4 curves at 512 Hz. The cows were kept free in individual pens (3 m × 3 m) during the recording.

The cows were moved and restrained in a pen used normally for veterinary purposes and prepared for the experiment.   The left side of the cows behind the shoulders was first shaved with clippers and afterwards with a manual razor.   The shaved area (left side 15 cm × 30 cm was cleaned with a liquid disinfectant.

The positive ECG electrode was placed on the left side of the cow over the heart area at the level of the elbow and over the 5th intercostal space, the negative electrode was placed 10 cm above it vertically, and the ground electrode was placed caudally of the horn base.

The used connection corresponds to the one used in the implantable device.

2.2 Cow's QRS-complex

The shape of the QRS-complex (Figure 1) depends on both the individual animal and the installation of the implant.   The Q-wave was not detectable in any of our measurements but to avoid confusion we still use the well-established abbreviation "QRS".   The R-wave, when present at all, is also too weak to be distinguished from relaxation waves such as the T-wave, which is higher in amplitude.   In some cows the R-wave did not rise above the noise level at all.   The S-wave is the most specific component of the ECG data and was thus chosen as the target for the detection algorithm. Similar observations and thorough explanations on lactating Holstein cow ECG can be found in (Deroth, 1980).   This is why we refer to the SS-interval instead of the commonly used term "successive RR-interval" (Tiusanen et al., 2015).
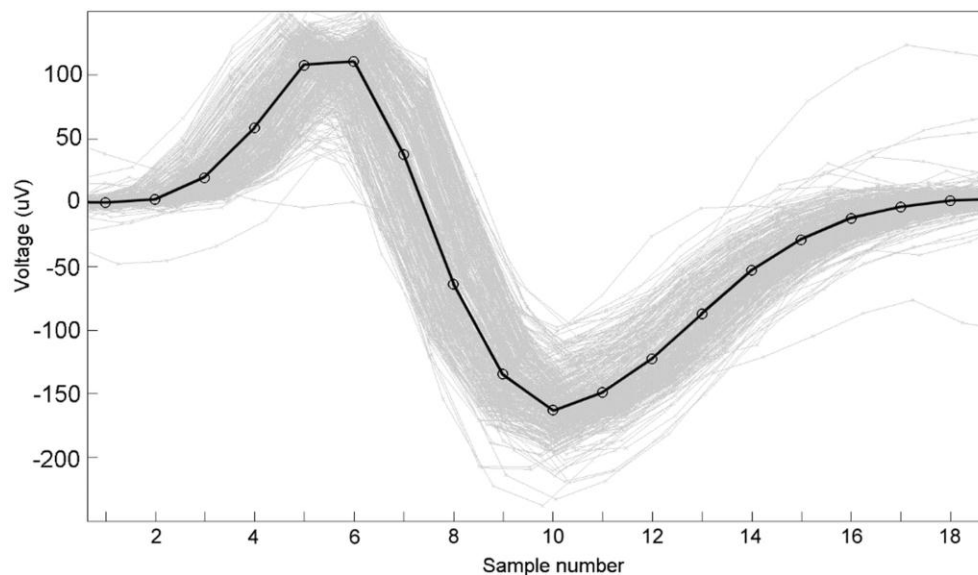

Figure 1 One cow's QRS-complex as an average of 100 detected heart beats measured at 256 Hz

2.3 The algorithm

The intended embedded platform would allow quite heavy calculations, but we decided to apply only multiplication, division, addition, subtraction and logical conditions in order to serve even lower-level future devices.

A simple pace error detector assisted us during algorithm development and parameter tuning by giving a preliminary count of detection errors.   The final evaluation was performed by counting and classifying every heart beat manually.

Both the amplitude and the baseline of our ECG recordings were unstable.   Reliable S-peak detection required an adaptive algorithm.   Therefore the algorithm includes simple amplitude monitoring and baseline tracking.

2.3.1 Amplitude monitoring

The amplitude A (μV) was calculated as the difference between the highest positive and the lowest negative voltage values by Equation (1) whenever a new voltage sample V_{NEW} is measured.

$$\begin{cases} V_{MAX} = \max(V_{NEW}, V_{MAX}) \times (1 - 1/f) \\ V_{MIN} = \min(V_{NEW}, V_{MIN}) \times (1 - 1/f) \\ A = (1 - 1/f) \times A_{OLD} + (1/f) \times (V_{MAX} - V_{MIN}) \end{cases} \quad (1)$$

where V_{MAX} is the positive and V_{MIN} the negative envelopes, A_{OLD} the previously calculated amplitude value (μV) and f the sampling frequency (Hz).

The envelope values are multiplied by $1 - 1/f$ to give them a sampling frequency independent 2.2 s fall time towards zero.   The old amplitude value A_{OLD} has the weight $1-1/f$ over the present envelope difference weight $1/f$.   Thereby A moves towards the present envelope difference value with a 2.2 s fall time (Figure 2).
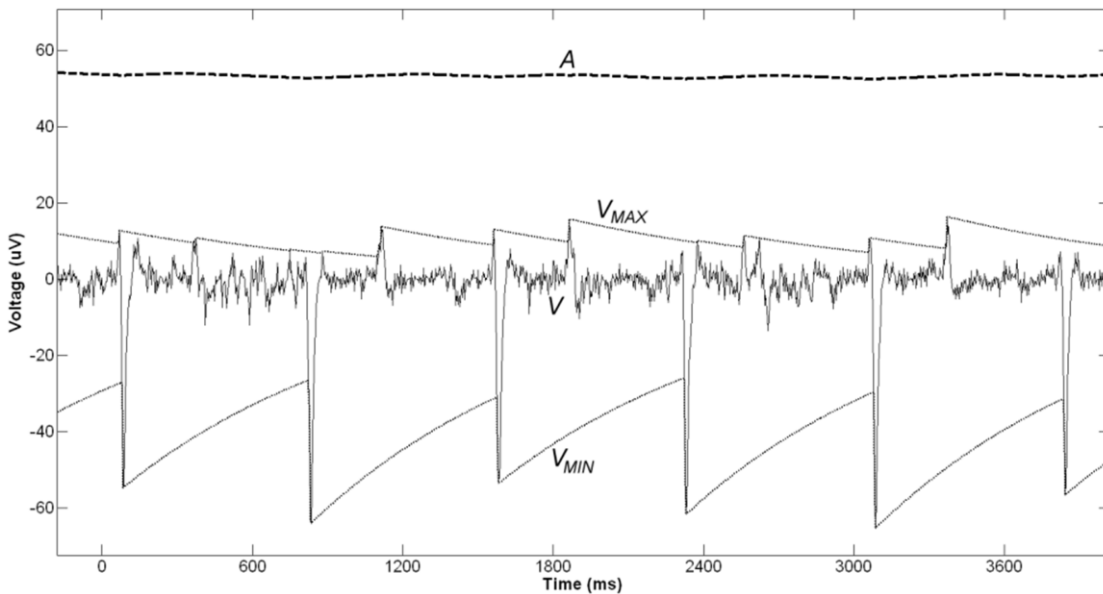

Figure 2   ECG signal V, positive V_{MAX} and negative V_{MIN} envelopes and the resulting amplitude A

2.3.2 Signal normalization

The baseline tracker is a custom high-pass filter, which simultaneously increases the signal dynamics and calculates the baseline B by the four steps in Equation (2).

$$\begin{cases} d_V = p_V \times (V_{NEW} - V_{OLD})^2 \times f / A \\ \Delta_B = p_B \times (V_{NEW} - V_{OLD}) / d_V \\ B = B_{OLD} + \Delta_B \\ V_{NORM} = V_{OLD} - B \end{cases} \quad (2)$$

where d_V is the amplified square of the derivate, p_V the amplification coefficient for the difference, V_{NEW} and V_{OLD} the newest and previous voltage sample values (μV) respectively, f the sampling frequency (Hz), A the amplitude (μV), ΔB the step change in the baseline (μV), B and B_{OLD} the present and previous baselines (μV) respectively and V_{NORM} the normalized voltage sample (μV).

Fast changes in V_{NEW} input result in a high d_V value which forces ΔB close to zero and the baseline level B will not change.   On the other hand, B level will follow all slow V_{NEW} changes (Figure 3).   Appropriate tuning of coefficients p_V and p_B produce a V_{NORM} curve where the QRS-complex remains sharp but most of other waves are attenuated (Figure 4).
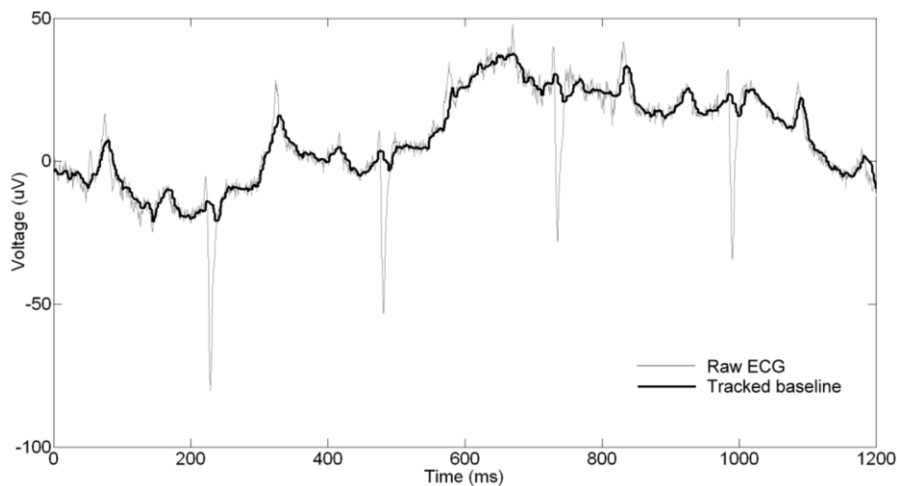
Figure 3   The raw ECG input V_{NEW} and the tracked baseline B.

In some occasions the input V changes very little, d_V gets values close to zero, ΔB becomes excessively high and produces a large step in B. For this reason we limited ΔB to 5% of the amplitude per sample. This value does not affect filter response but prevents undesired steps in B when unpredicted cases such as disturbance in the signal occur.
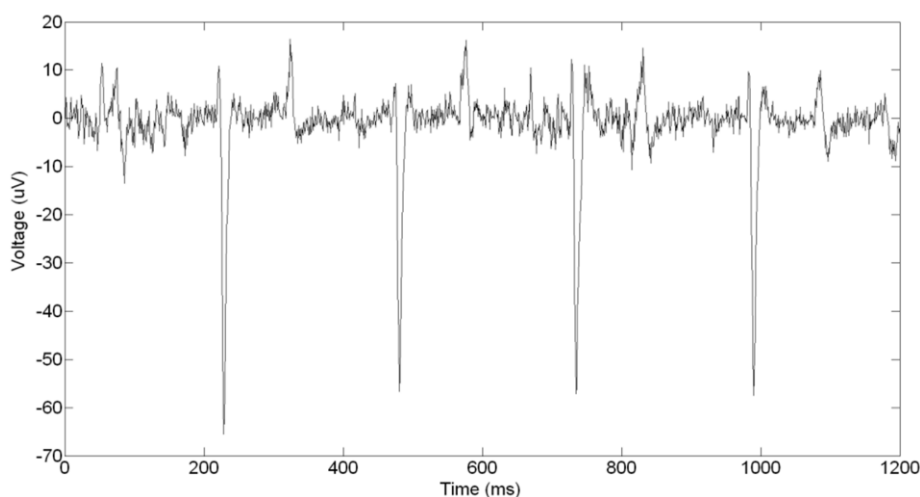

Figure 4 The normalized V_{NORM} of the ECG data in Figure 3

2.3.3 S-peak detection trigger

The actual triggering of the S-wave is a difference formula similar to those evaluated in (Friesen et al. 1990). A one-sample difference is too sensitive to noise and causes false alarms. The duration of the falling S-wave for a cow (as seen in Figure 1) is 15-18 ms. We found 15 ms to be the best differencing time to detect the S-wave reliably but to not react on noise or T-waves. At our sampling frequency 256 Hz this means differencing over 4 samples. This interval must be adjusted for every f.

The S-wave trigger T is the square of the difference over four samples d_T in relation to the amplitude A in Equation (3). Squaring improves dynamics which reduces false trigs. For our data, the S-wave has started when $T > 0.02$.

$$\begin{cases} d_T = \left(V_{NORM\,(i)} - V_{NORM\,(i-4)} \right)/4 \\ T = \left(d_T / A \right)^2 \end{cases} \quad (3)$$

2.3.4 Peak location search time

Once the condition $T > 0.02$ is met, the algorithm will keep searching for the lowest V_{NORM} value for 300 ms. This search time allows a heart rate as high as 200

beats/min without multiple S-waves occurring during the search.   The search time is not critical to the algorithm performance, but a long search is beneficial in noisy signal analysis since it gives the algorithm the opportunity to find the S-wave bottom peak even if triggered by a false T alarm. On the downside, if noise amplitude exceeds the signal, faulty peaks will be detected.   Once the peak is detected, new triggering is prohibited until 300 ms has elapsed from the S-wave peak.

2.4 Validation

We developed the algorithm using complete ECG curves from 11 individual cows and by programming the detector into a MATLAB graphical user interface.   The

detector errors were divided into four categories, which are presented in the examples in Figure 5.

Since the primary application will be the comparison of lying time HRV we recorded 14 complete 10 min ECG curves from 10 individual cows during lying time.   10 curves were recorded at 256 Hz and 4 curves at 512 Hz. After executing the detector program we counted all detection errors and classified them according to Figure 5. The errors were found from the large data by evaluating every peak where the successive SS-interval was more than 30 ms.   Most of these peaks were correctly detected, but this approach reduced the amount of hand work.
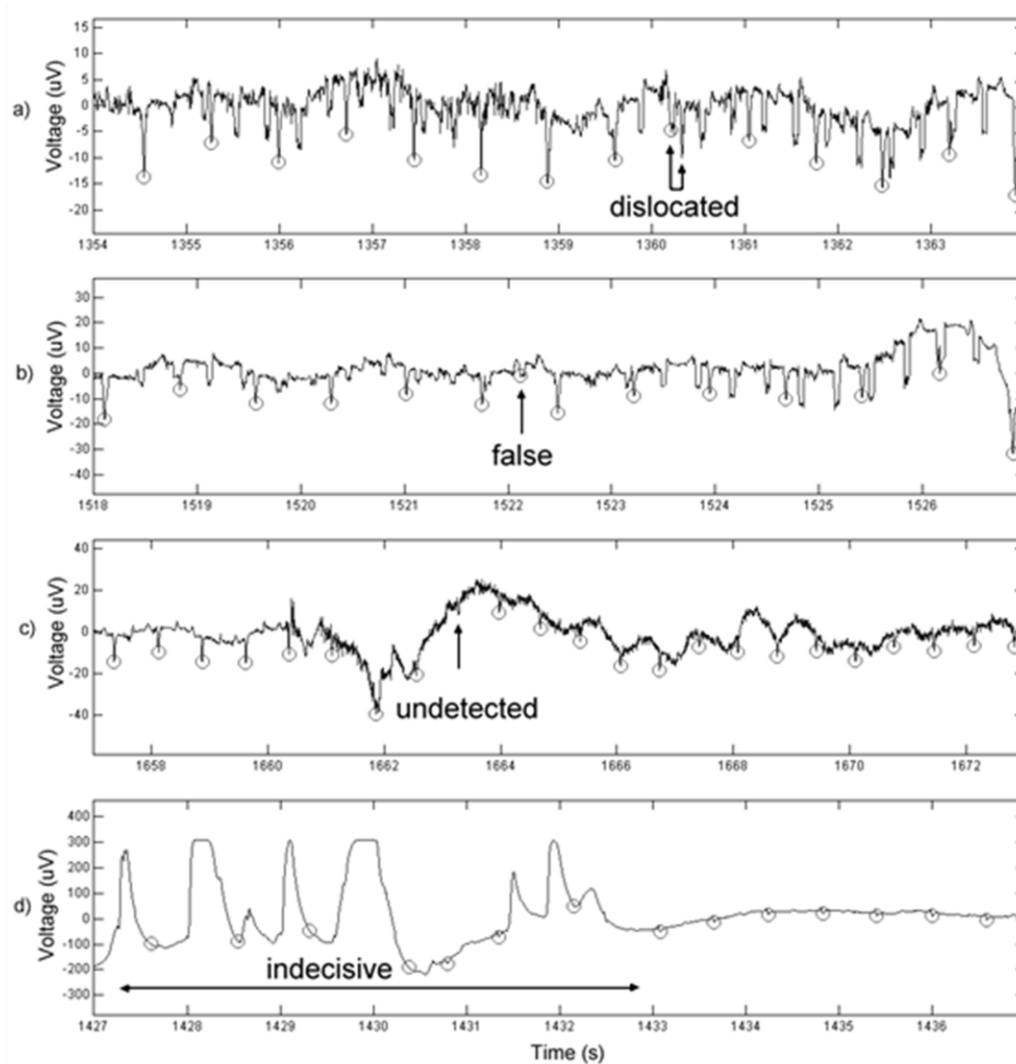
(a)   the peak location is dislocated; (b) one false peak is detected; (c) peak is completely undetected; (d) many peaks are indecisive on whether the detector works correctly or not

Figure 5 Detector error classification

The detector performance was also evaluated during cow's free movement in an individual pen. All the examples in Figure 5 are from these recordings. The baseline would shift up to 10 amplitudes during only a few heart beats but always returned to the zero level. Since the baseline shifts clearly hampered the detector performance, we evaluated 20 such cases and classified the baseline shift speed visually as in Figure 6 in order to estimate the baseline shift influence on detection errors.
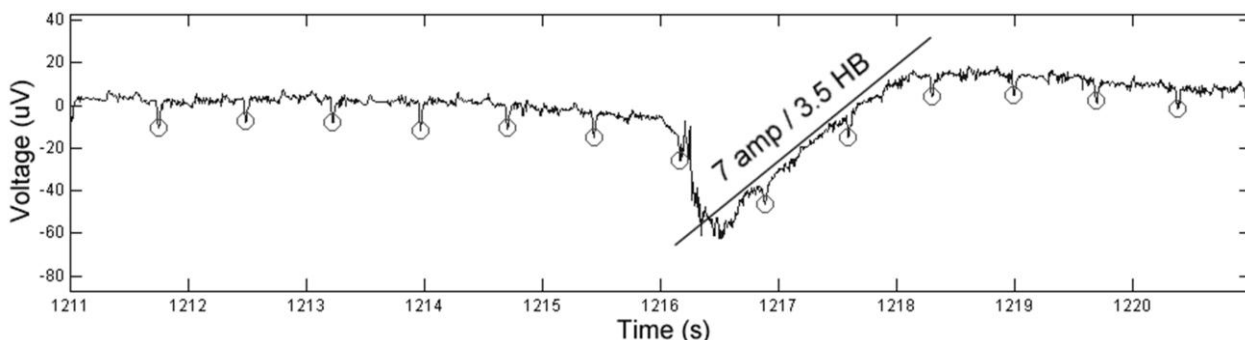

Figure 6 Example of baseline shift speed, which is 2 amplitudes per beat interpreted visually from the data

Our device also picked up different kinds of interference. In Figure 5 the RFID reader induction pulses can be noticed in the right hand part in Figures 5a and 5b. Where the pulses were higher in amplitude than the actual S-waves, they corrupted these periods of the data into the indecisive category. These sections of data were not evaluated in detail.

Table 1 presents the results from the error calculations. The detector algorithm performs very well on the lying time ECG. Only 7 of all the 5115 heart beats were misinterpreted. The performance becomes much worse once the cows start moving in the barn. An average 3.7% of the heart beats go wrong, when the indecisive beats are excluded.

3   Results

Table 1 ECG detection algorithm validation results

Behaviour	Cow name	f, Hz	Heart beats	Number of errors				Error probability, %
				Dislocated	False	Undetected	Indecisive	
Lying	Triumpf	256	427	1	0	0	0	0.23
	Triumpf	256	428	1	0	0	0	0.23
	Tussaud	256	778	0	0	0	0	0.00
	Unikko1	256	469	0	0	0	0	0.00
	Unikko2	256	509	0	0	1	0	0.20
	Unikko2	256	480	1	0	1	0	0.42
	Unikko2	256	495	0	0	1	0	0.20
	Viennetta1	256	406	0	0	0	0	0.00
	Viennetta1	256	366	1	0	0	0	0.27
	Viennetta2	256	380	0	0	0	0	0.00
	Viennetta2	256	377	0	0	0	0	0.00
Moving	Anna	512	814	12	12	4	1	3.56
	Ceres	512	625	2	10	26	2	6.40
	Maja	512	733	9	13	1	0	3.14
	Martha	512	824	4	5	42	0	6.19
	Tavernessa [1]	256	1588	11	2	1	20	0.89
	Tavernessa [2]	256	2449	89	11	6	17	4.36

Note: 1) 20 min of quite noisy data.   2) 30 min of very noisy data

According to the simple baseline shift test (Figure 7) a shift slower than 1 amplitudes per heart beat causes errors only randomly.   When the baseline shifts faster than 2 amp/HB, it is likely for the detector to make one or several errors.
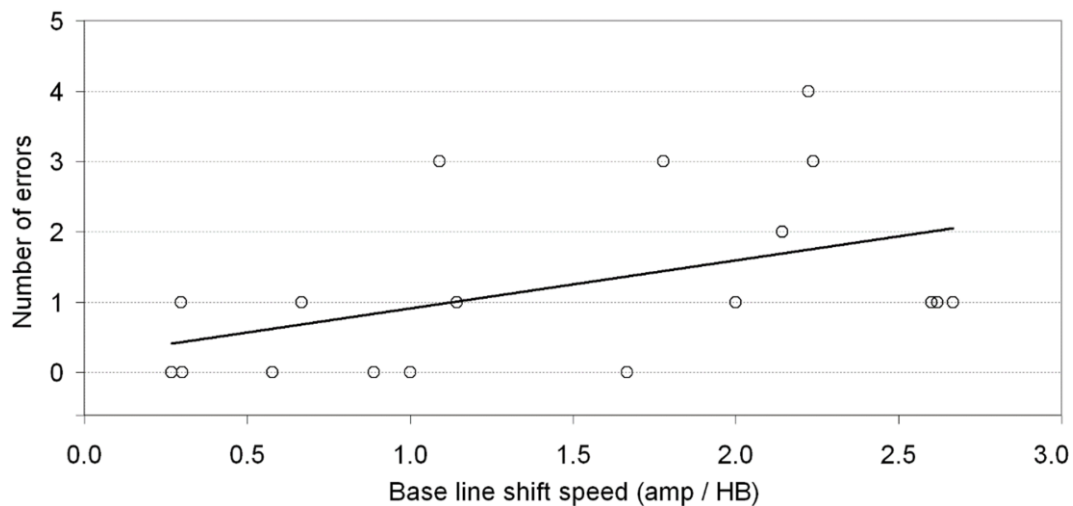

Figure 7 Detection error probability and linear regression when there are fast shifts in ECG baseline

4   Discussion

We have successfully developed a new algorithm for detecting beat-to-beat intervals from cattle ECG that can run on a resource constrained implant.   The algorithm performs well during rest, but the detection performance decreases on surface recordings during movement.   The developed algorithm worked for all of the tested cows, whereas the tested human algorithms from Friesen et al. (1990) were completely unable to detect the R or S wave for most of the animals in the dataset.

We found that the amplitude of the R-peak in cow ECG is very small as compared to humans.   This is in accordance to the findings in (Tiusanen et al. 2015; Marques, 2008; Rezakhani, 1980).   Therefore we focused on detecting the SS-interval which is a lot less susceptible to noise.

Eventually the changes in HRV will be monitored by comparing measurements during cow's lying times.   This excludes many problems concerning muscular EEG interference and sensor movement.   Therefore the detector algorithm was primarily validated using ECG data measured from lying animals. Further, the implant measurements have less noise than surface measurements that were used for the algorithm development.

The d_T could be restricted to negative values, but we did not find it necessary.   A noise figure could be used to adjust T threshold and search time.

In noisy conditions a too fast drop in V could be excluded from triggering the search, since it probably is distortion instead of an S-wave.   This would still not help detecting a heartbeat occurring simultaneously with the disturbance.

5   Conclusions

The developed algorithm can be used to record beat-to-beat intervals from adult cows in real time using an implantable ECG monitor. The algorithm is included in MATLAB based graphical user interface for simple use in animal welfare research.

References

Chen, W., N. Tetsu, T. Kobayashi, T. Saito, E. Kasuya, and Y. Honda.   2000.   ECG and heart rate detection of prenatal

cattle foetus using adaptive digital filtering. *In Proc. 22nd Annual International Conference of the IEEE*, 2:962-965. Engineering in Medicine and Biology Society.

DeRoth, L. 1980. Electrocardiographic Parameters in the Normal Lactating Holstein Cow. *Canadian Veterinary Journal*, 21(10): 271–277.

Friesen, G. M., T. C. Jannett, M. A. Jadallah, S. L. Yates, S. R. Quint and H. T. Nagle. 1990. A Comparison of the Noise Sensitivity of Nine QRS Detection Algorithms. *IEEE Transactions on Biomediacal Engineering*, 37(1):85–98.

Frondelius, L., K. Järvenranta, T. Koponen, and J. Mononen. 2015. The effects of body posture and temperament on heart rate variability in dairy cows. *Physiology and Behavior* 139:437-441.

Gygax, L., I. Neuffer, C. Kaufmann, R. Hauser, and B. Wechsler. 2008. Restlessness Behaviour, Heart Rate and Heart-Rate Variability of Dairy Cows Milked in Two Types of Automatic Milking Systems and Auto-Tandem Milking Parlours. *Applied Animal Behaviour Science*, 109(2-4):167-179.

Hagen, K., J., Langbein, C. Schmied, D. Lexer, and S. Waiblinger. 2005. Heart Rate Variability in Dairy cows—influences of Breed and Milking System. *Physiology and Behavior*, 85(2):195-204.

Jane, R., P. Laguna, N. V. Thakov, and P. Caminal. 1992. Adaptive Baseline Wander Removal: Comparative Analysis With Cubic Spline Technique (Published Conference Proceedings style), in *Proc. IEEE Computers in Cardiology*. Durham, pp. 143–146.

Marques. F. J. 2008. Cardiac arrhythmias in large animal species: Is it worth worrying about? *Large Animal veterinary rounds* 8(5): 1-6.

Rezakhani, A., A. A. Paphan, and S. Shekarfroush. 2004. Analysis of base apex lead electrocardiograms of normal dairy cows. *Veteniarski arhiv*, 74(5): 331–358.

Riistama, J., and T. Vuorela. 2011. Implantable measurement device to assist in determining the psychophysiological well-being of dairy cattle, Presented at the Biomed 2011 *Int. Conf. Biomedical Engineering*, Innsbruck, Austria.

Stewart, M. J., M. Stookey, K. J. Stafford, C. B. Tucker, A. R. Rogers, S. K. Dowling, G. A. Verkerk, A. L. Schaefer, and J. R. Webster. 2009. Effects of Local Anesthetic and a Nonsteroidal Antiinflammatory Drug on Pain Responses of Dairy Calves to Hot-Iron Dehorning. *Journal of Dairy Science*, 92(4): 1512-1519.

Tiusanen, M. J., M. I. Hautala, E. M. Ternman, and M. E. Pastell. 2015. Geometrical method for interpolating S-peaks from cow ECG using a microcontroller. *Biosystems Engineering*, 129: 324-328.

von Borell, E. J. Langbein, G. Després, S. Hansen, C. Leterrier, J. Marchant-Forde, R. Marchant-Forde, M. Minero, E. Mohr, A. Prunier, D. Valance, and I. Veissier. 2007. Heart rate variability as a measure of autonomic regulation of cardiac activity for assessing stress and welfare in farm animals — A review. *Physiology and Behavior*, 92(3): 293-316.